

Generating an adjustable three-dimensional dark focus

Dvir Yelin, Brett E. Bouma, and Guillermo J. Tearney

Harvard Medical School and the Wellman Center for Photomedicine, Massachusetts General Hospital,
55 Fruit Street, BAR 703, Boston, Massachusetts 02114

Received November 6, 2003

Conditions for generating a dark focus surrounded by light in all three dimensions are presented. A simple technique for generating such a dark region is demonstrated experimentally. The method is compared with previous attempts at creating a three-dimensional dark focus. © 2004 Optical Society of America

OCIS codes: 020.7010, 220.2560.

A dark spot surrounded by regions of high light intensity is desirable for applications such as optical tweezers and atom trapping. High- and low-index particle lateral trapping was demonstrated¹ and analyzed² with a doughnut-shaped beam, where the dark focus was surrounded by light in the lateral dimensions. Several techniques for generating a dark focus surrounded by light from all directions (three-dimensional dark focus) that were recently described used special phase³ and amplitude⁴ masks and a spatial light modulator.⁵ In this Letter we present a simple criterion for the existence of a dark focus, propose an optical setup for generating a three-dimensional dark focus, and compare our method with two recently described^{3,4} techniques for generating a three-dimensional dark focus.

Assuming paraxial approximation, the field at the focal point of an aberration-free lens system is directly proportional to the zero spatial frequency component of electric field E . The condition for zero intensity at the focal point is therefore

$$\int_S E_i ds = 0, \quad (1)$$

where S denotes the area of the lens aperture and i represents each of the two transverse coordinates. This condition implies that every optical beam with a zero dc component will generate a dark focus. This condition, however, is not satisfactory for the existence of a dark focus that is surrounded by light from all directions. For example, the doughnut beam^{1,2} satisfies Eq. (1) but provides confinement along only the lateral dimensions of the focused beam. Three-dimensional dark focus requires a structurally unstable beam that cannot be obtained with a single propagation mode. Only interplay between two or more structurally stable propagation modes, with two or more of the modes having nonzero on-axis intensity and different Guoy phase shifts,⁶ can produce a three-dimensional dark focus. Let us assume, for simplicity, a monochromatic, radially symmetric field distribution. The field amplitude $U(r, z)$ can be expanded in terms of Laguerre–Gauss (LG) modes with zero azimuthal mode index $u_p^0(r, z)$. The field amplitude on the optical axis $U(r = 0, z)$ is the sum of all the on-axis amplitudes of the (structurally stable)

LG modes:

$$U(0, z) \propto \sum_p a_p A_p \exp[i\psi_p^G(z) + i\phi_p],$$

where a_p is the expansion coefficient of the LG mode u_p^0 , A_p is a normalization constant, ϕ_p is the planar phase of the mode, and ψ_p^G is its Guoy phase. Variations in the field amplitude along the optical axis are due to the Guoy phase. A three-dimensional dark focus occurs where $U(0, 0) = 0$ and where $U(0, z') \neq 0$ for some $z = z'$, where $z' \neq 0$. The radial and the axial symmetry around the focal point $z = 0$ ensure that the on-axis out-of-focus light will surround the dark focal point from all directions. These conditions for a three-dimensional dark focus imply that generating a dark trap is straightforward: Any monochromatic, radially symmetric beam, with nonzero on-axis intensity at some point along the optical axis, that satisfies Eq. (1) generates a three-dimensional dark focus. The dimensions, geometry, and depth of the three-dimensional dark focus can vary for a given choice of field distribution at the far field.

In the experiment by Arlt and Padgett⁴ that demonstrated the generation of the optical bottle beam by use of a diffractive optical element (DOE), a three-dimensional dark focus was obtained by the interference of two structurally stable beams with a π phase difference in both the Guoy and planar phase terms. A sketch of the cross section of the resulting beam after the DOE is plotted in Fig. 1a (solid curve) with the two LG modes that form it (dotted curves). The beam satisfies Eq. (1) and exhibits nonzero axial intensity at one Rayleigh range from the focal point. DOEs allow for simple and compact optical setup; however, the fabrication of these devices requires expertise in fabricating high-efficiency diffractive optics. Stray light from the hologram reduces the contrast of the dark focus but can be minimized by improvements in the photographic process.⁴

In an experiment by Ozeri *et al.*,³ in which the dark focus was used to trap atoms, Eq. (1) was satisfied by means of a phase mask. After the mask, the beam has its maximum intensity on the optical axis. A sketch of the cross section of the field after the mask is shown in Fig. 1b (solid curve) with the beam profile before

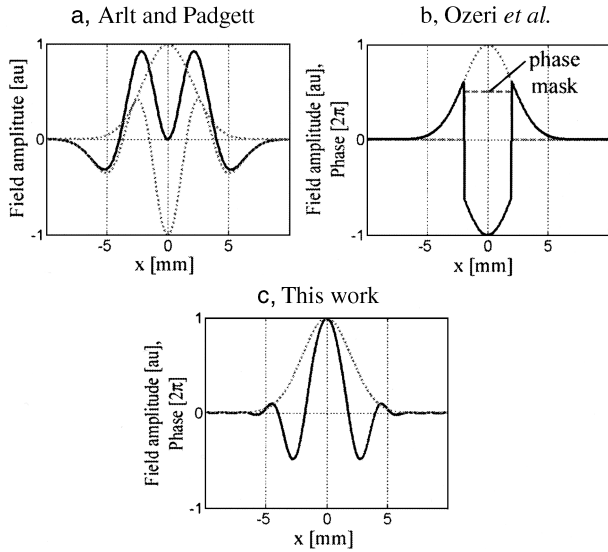


Fig. 1. Comparison of three techniques for generating dark focus: a, use of an amplitude hologram (data taken from Ref. 4); b, use of a phase element placed in the beam's optical path (data taken from Ref. 3); c, use of two interfering beams with different curvatures. The far-field distribution for each method was calculated assuming a Gaussian-shape generating beam with $\sigma = 2$ mm.

the mask (dotted curve) and the phase change induced by the mask (dashed line). This technique produces a three-dimensional dark focus with low stray light. The phase mask itself is designed for a specific wavelength and beam geometry and can be fabricated by use of a commercial optical coating machine. Like the dark focus produced by DOEs, the phase mask allows for a compact optical setup.

We propose another method for generating a three-dimensional dark focus with off-the-shelf optics that can be manipulated in real time to change the properties of the focused beam. Consider two identical Gaussian beams, with opposing radii of curvature, focused by a lens. We can write the expression for the total field before the lens as

$$\begin{aligned}
 E &\propto \text{Re} \left[\exp\left(-\frac{r^2}{2\sigma^2}\right) \exp\left(\frac{ikr^2}{2\delta_1}\right) \right. \\
 &\quad \left. + \exp\left(-\frac{r^2}{2\sigma^2}\right) \exp\left(\frac{ikr^2}{2\delta_2} + i\Delta\phi\right) \right] \\
 &= 2 \exp\left(-\frac{r^2}{2\sigma^2}\right) \cos\left(\frac{kr^2}{2\delta} + \frac{\Delta\phi}{2}\right), \quad (2)
 \end{aligned}$$

where σ is the transverse width of the beams, δ_1 and δ_2 are the effective focal distances of the two beams resulting from the small but opposite curvatures, $\delta_1 = -\delta_2 \equiv \delta$, $\Delta\phi$ is the planar phase difference between the beams, and $k = 2\pi/\lambda$, where λ is the wavelength. Substituting expression (2) into Eq. (1) yields

$$\int_0^a \exp\left(-\frac{r^2}{2\sigma^2}\right) \cos\left(\frac{kr^2\Delta f}{4f^2} + \frac{\Delta\phi}{2}\right) r dr = 0, \quad (3)$$

where a is the radius of the focusing lens clear aperture. We express δ in terms of the focal length of lens f and the separation between the two foci of beams Δf with the relation

$$\frac{1}{\delta} = \frac{1}{f} - \frac{1}{f + \Delta f/2} \approx \frac{\Delta f}{2f^2}, \quad \left(\frac{\Delta f}{2f} \ll 1\right).$$

By tuning each of the parameters (σ , f , Δf , and $\Delta\phi$) we can satisfy Eq. (3) and minimize the intensity at the focal point. A simulation of the cross section of the field in our experiment (solid curve) with the original Gaussian cross section of the two beams before interference occurs (dotted curve) is shown in Fig. 1c.

The optical setup for obtaining a three-dimensional dark focus is shown in Fig. 2. A beam from a He-Ne laser at a wavelength of $\lambda = 632$ nm is split into the two arms of a 50/50 Mach-Zehnder interferometer. The beam curvature on one arm is slightly changed by two lenses separated by a distance of $L = f_1 + f_2 + \epsilon$, where $f_1 = 100$ mm and $f_2 = 120$ mm are the focal lengths of lenses L1 and L2, respectively, and ϵ determines the final curvature of the beam. The distance between the lenses was tuned to separate the beam waists by two Rayleigh ranges, $\Delta f = 2Z_R$, and their focal lengths were chosen to maintain similar transverse beam widths at lens L3. A glass window is placed in the other arm of the interferometer to match the optical path length and to control phase difference $\Delta\phi$ between the two arms. The beam at the output of the interferometer is focused with lens L3, which has a focal length of $f_3 = 65$ mm and a clear aperture of $a = 10$ mm.

By solving the Fresnel integral, we simulated the optical field distribution around the focal region for the parameters of the experiment ($\lambda = 632$ nm, $f_3 = 65$ mm, $a = 10$ mm) and for a Gaussian intensity profile (TEM₀₀ mode) with $\sigma = 2.4$ mm. The field distribution in the x - z plane around the focal point for $\Delta\phi = 1.5\pi$ and $\Delta f = 2Z_R$ was calculated and is shown in gray scale in Fig. 3a, where high pixel values represent high field amplitudes. Field cross sections along the z axis, the x axis, and the diagonal, where the lowest point in the light wall around the focus is located, are shown in Figs. 3b, 3c, and 3d, respectively. The lowest point of the light wall has an intensity that is 0.27 of the maximum wall height along the z axis.

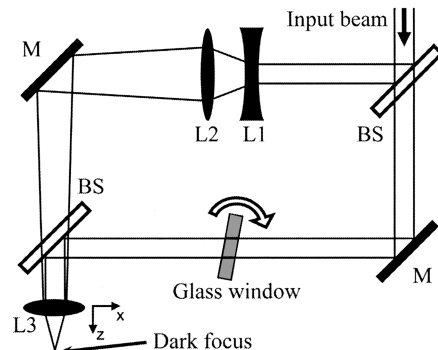


Fig. 2. Schematic of the optical setup for generating dark focus: M, mirror; BS, beam splitter.

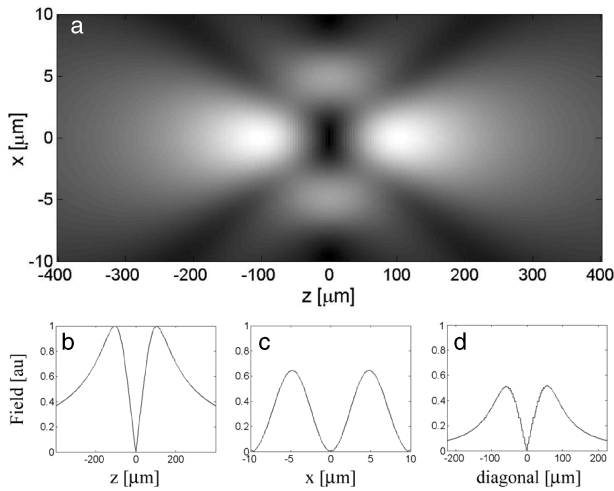


Fig. 3. (a) Simulation of the optical field distribution around the focal region. Field cross section along the (b) z axis, (c) x axis, (d) the diagonal.

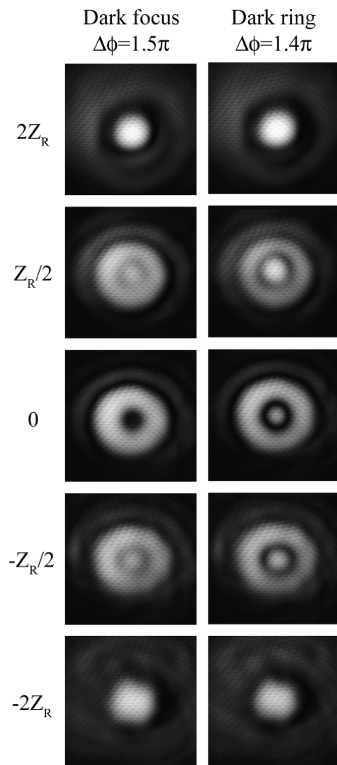


Fig. 4. Experimental results showing the transverse intensity cross section of the light for different locations along the z axis. The left column shows the light distribution for the dark focus ($\Delta\phi = 1.5\pi$), and the right column shows the light distribution of a dark ring ($\Delta\phi = 1.4\pi$).

Because of the complete destructive interference and the lack of stray light, the light intensity at the focal point is identically zero; thus the height of the light barrier is determined by the laser intensity only.

To demonstrate the generation of a dark focus, we imaged the focal region of lens L3 (see Fig. 2) with a $40\times$ objective and a CCD camera. The phase dif-

ference, $\Delta\phi$, between the two arms of the interferometer was adjusted to obtain the dark focus. The beam transverse intensity profiles at $z = 2Z_R$, $Z_R/2$, 0 , $-Z_R/2$, and $-2Z_R$, where Z_R is the Rayleigh range, are shown in the left column of Fig. 4. These profiles agree well with the simulated field distribution in Fig. 3.

The optical setup provides some flexibility in optimizing and manipulating the intensity distribution at the focus. For example, slightly tilting the glass window allows the phase difference between the two beams to be adjusted to $\Delta\phi = 1.4\pi$ to obtain a dark ring around a bright focal region. Similar to the dark spot, the ring is also completely surrounded by light, although the light wall along the diagonals is slightly lower. The ring diameter can be continuously tuned to a certain extent by tilting the glass window. The dark ring might be useful in controlling the interaction area between the laser beam and low-index particles in optical tweezers. A tunable-sized dark ring might also allow for fine tuning the geometric shape of an atom trap (see, for example, Ref. 7).

In this Letter we have presented the conditions for generating dark focus and have shown that previous attempts at generating dark focus satisfy these conditions. The new technique demonstrated here also satisfies these conditions, uses off-the-shelf components, can be easily tuned to different wavelengths, and allows for dynamic control over the shape of the dark region. The use of an interferometric technique, however, imposes requirements on component stability that are not present for other techniques. In our experiment we used a compact design for the interferometer, which helped reduce mechanical drift. In future iterations of this method a compact interferometer design with a closed-loop feedback stabilization system could significantly improve the darkness at the focus by optimizing the system's long- and short-term stability.

This research was supported in part by National Science Foundation award BES-0086709, the Department of Defense Medical Free-Electron Laser Program, the Whitaker Foundation, and a generous gift from Dr. and Mrs. J. S. Chen to the optical diagnostics program of the Massachusetts General Hospital Wellman Center for Photomedicine. D. Yelin's e-mail address is dyelin@partners.org.

References

1. M. Reicherter, T. Haist, E. U. Wagemann, and H. J. Tiziani, *Opt. Lett.* **24**, 608 (1999).
2. D. W. Zhang and X.-C. Yuan, *Opt. Lett.* **28**, 740 (2003).
3. R. Ozeri, L. Khaykovich, and N. Davidson, *Phys. Rev. A* **59**, 1750 (1999).
4. J. Arlt and M. J. Padgett, *Opt. Lett.* **25**, 191 (2000).
5. D. McGloin, C. C. Spalding, H. Melville, W. Sibbett, and K. Dholakia, *Opt. Commun.* **225**, 215 (2003).
6. J. Courtial, *Opt. Commun.* **151**, 1 (1998).
7. A. Kaplan, N. Friedman, M. Andersen, and N. Davidson, *Phys. Rev. Lett.* **87**, 274101 (2001).